



HAL
open science

Phenotypic characterization of organoids derived from pig intestine segments

F. Blanc, M. Mongellaz, F. Pepke, C. Bevilacqua, J. Riviere, M. Vilotte, E. Giuffra, Giorgia Egidy

► **To cite this version:**

F. Blanc, M. Mongellaz, F. Pepke, C. Bevilacqua, J. Riviere, et al.. Phenotypic characterization of organoids derived from pig intestine segments. Wageningen Academic Publishers, pp.2097-2100, 2022, 978-90-8686-940-4. 10.3920/978-90-8686-940-4_505 . hal-04231354

HAL Id: hal-04231354

<https://hal.inrae.fr/hal-04231354v1>

Submitted on 6 Oct 2023

HAL is a multi-disciplinary open access archive for the deposit and dissemination of scientific research documents, whether they are published or not. The documents may come from teaching and research institutions in France or abroad, or from public or private research centers.

L'archive ouverte pluridisciplinaire **HAL**, est destinée au dépôt et à la diffusion de documents scientifiques de niveau recherche, publiés ou non, émanant des établissements d'enseignement et de recherche français ou étrangers, des laboratoires publics ou privés.

Phenotypic Characterization of Organoids Derived from Pig Intestine Segments.

F. Blanc*, M. Mongellaz, F. Pepke, C. Bevilacqua, J. Riviere, M. Vilotte, E. Giuffra* and G. Egidy

Université Paris-Saclay, INRAE, AgroParisTech, GABI, 78350, Jouy-en-Josas, France;

* fany.blanc@inrae.fr; elisabetta.giuffra@inrae.fr

Abstract

Organoids (“mini-organs”) derived from adult stem cells residing in tissues can provide near-physiological *in vitro* “Reduction, Refinement, and Replacement (3Rs)” models for genotype-to-phenotype research in animal sciences. Our aim was to assess the effective ability and reliability of pig intestinal organoids to reflect the phenotypes of the specific gut portion they are derived from. To this issue we generated organoids from the small intestine (duodenum, jejunum, ileum) and colon from cryopreserved biopsies of four Large White pigs after adapting the protocol to commercial slaughter conditions and further standardization of lab culture and phenotyping procedures. Here we report the comparison of organoids cultured in three and two dimensions (3D and 2D) *vs.* the original animal tissue in terms of morphology, number and growth rate, cell composition and barrier tissue integrity, and highlight the main organoid *vs.* tissue specificities.

Introduction

Organoids (“mini-organs”) can be obtained from embryonic cells, induced pluripotent stem cells and adult stem cells (from tissue biopsies of almost any organ and animal species). They are easily biobanked and amenable to many biochemical and genetic perturbations (Clevers, 2016). Gut organoids derived from intestinal crypts retain some of the key morphological and molecular features of the specific gut segment they derive from and are increasingly used in several farmed species, including pigs (Li *et al.*, 2019; van der Hee *et al.*, 2020).

Organoids are regarded as promising, near-physiological *in vitro* “3Rs” models for genotype-to-phenotype research, e.g. to study in highly reproducible conditions how genetic variation may affect key cellular processes underlying complex traits relevant for sustainable productions (Clark *et al.*, 2020). However, little is known so far on the relative influence of experimental and biological factors on organoid phenotypes. Specific culture conditions, passaging and culturing time can change the cellular state within the organoids. Recent analyses of transcriptional variance in organoids derived from human biopsies pointed to the heterogeneity of cohorts, organoids production and growth (Criss *et al.*, 2021; Gehling *et al.*, 2021, Mohammadi *et al.*, 2021).

Our global aim is to assess to what extent porcine gut organoids derived from different segments of the small intestine (duodenum, jejunum, ileum) and colon recapitulate the phenotypic variability of the tissue they are derived from, with a focus on phenotypes involving gut innate immunity responses. We report here the morphology, number and growth rate, cell composition and barrier tissue integrity phenotypes of these multiple organoids in comparison to the original tissue as a result of their production and culture in our laboratory standardized conditions. These results paved the basis of a transcriptome study in progress.

Materials & Methods

Generation and culture of pig 3D and 2D organoids from frozen tissues. Pig intestinal organoids were generated from cryopreserved intestinal biopsies of four 5-month-old biobanked Large White pigs as described (Beaumont *et al.*, 2021). Cell number was adjusted at each passage (10,000 cells seeded in 50 μ L droplets with 6-8 mg/mL of Matrigel (Corning, ref 356231) in 24-well plates) with basal culture medium (BCM) (van der Hee *et al.*, 2018). Conditioned media were from the same batches and their optimal concentrations were experimentally tested. To obtain 2D layers, organoids were processed to obtain single cell suspensions, 30,000 cells were seeded on Transwells with 0.4 μ m pore polycarbonate membrane inserts (Corning) or 96-well plates (Corning) pre-coated with 0.5% (v/v) Matrigel, and cultured in BCM supplemented with 10 μ M Y27632 at first. BCM was then refreshed every 2 or 3 days until cells reached around 75% of confluence. Medium was then replaced by differentiation medium (BCM without Wnt3A conditioned medium) for 3 days. The Transepithelial electrical resistance (TEER) was assessed using the Epithelial Volt/Ohm Meter EVOM2 (WPI) on Transwells at confluence.

Evaluation of 3D & 2D organoid growth rate and count. Phase contrast microscopy images of developing 3D organoids at 5, 6 and 7 days of culture were obtained with a PlanApoN 2x objective. Organoids area and count were estimated by image analysis using Fiji (particles > 2000 μ m² and circularity between 0.2 and 0.9 were kept for the analysis). Confluence of 2D layers was also estimated by image analysis with Fiji from daily-acquired phase contrast microscopy images.

Histology and immunohistochemical staining. Tissues and organoids in 3D and 2D-layers (insert membranes) were fixed in paraformaldehyde 4% for 1h and paraffin-embedded; 5 μ m-sections were stained by hematoxylin-eosin-saffron (HES) or alcian blue/periodic acid Schiff, or with antibodies to detect chromogranin A (Novus biological, ref NBP2-34240), villin-1 (Novus biological, ref NBP1-85335), β -catenin (Novus biological, ref NBP2-34240), and occludin (ThermoFisher, ref 71-500). Detection was then performed with goat anti-rabbit IgG-AF647 (ThermoFisher, ref A-21245) and goat anti-mouse IgG-AF555 (ThermoFisher, ref A-21422) and DAPI as nuclear counterstaining. Images acquired with a digital slide scanner (Pannoramic SCAN, 3DHISTECH), objective 20x were analyzed using CaseViewer and QuantCenter softwares (3DHISTECH).

Statistical analyses. Data analyses were performed using R (v4.1.0). Principal Component Analyses (PCA) were performed using FactoMineR (v2.4) package using the imputePCA function of missMDA (v1.18) package to handle missing values, and visualized with the factoextra R package (v1.0.7).

Results and Discussion

Optimized protocols for porcine tissue collection & 3D/2D gut organoid culture. We have optimized existing protocols to directly cryopreserve human intestinal tissues allowing to generate organoids after thawing (Tsai *et al.*, 2018) for the four gut regions (duodenum, jejunum, ileum and colon) from 4 Large White pigs at slaughter age. This method allows sampling and storing of a large number of animal samples at once, which would not be compatible with immediate labor-intensive organoid culture. In addition, this procedure has guaranteed organoid culture generation free from bacterial and fungal contaminations. We then progressed in the establishment of standardized protocols to grow organoids optimizing reproducibility. We found that mechanical and enzymatic digestions performed at each

passage reduced the heterogeneity in organoid stages within the same culture. We also set up a fixed number of cells to seed at each passage and a weekly passaging frequency. For 2D gut organoid cultures, we have standardized the number of cells seeded in each well and evidenced a variability concerning the time needed to reach 75% of confluence (ranging from 5 to 9 days).

In those conditions, area of organoids doubled (mean $\times 2.1$) from 5 to 7 days while their circularity decreased (means 0.679 after 5 days vs. 0.618 after 7 days). Differences between the original gut segment organoids were derived from, could be revealed in terms of morphology (colon organoids were bigger and duodenum ones less circular) and density in cultures (higher for duodenum organoids and lower for ileum ones). We also observed a variability of organoid density within pigs. Morphology and structure of organoids in both 3D and 2D resembled that of gut tissues. Labelling of goblet cells, mature enterocytes and neuroendocrine cells was in accordance with the original tissues (Figure 1).

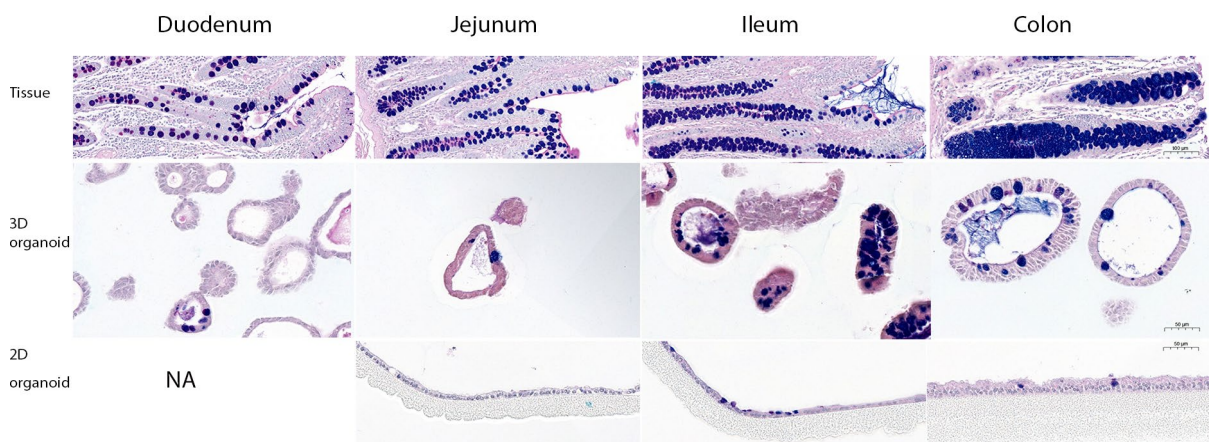


Figure 1. Representative alcian blue/periodic acid Schiff staining of gut tissues, 3D and 2D organoids for duodenum, jejunum, ileum and colon. NA: not yet available

Pig gut organoids retain original tissue characteristics. Gut tissues clearly clustered by the corresponding gut regions in a PCA analysis performed with the different histological and immunohistochemical phenotypes measured (Figure 2A). The four gut regions spread along the first dimension in the gut tract order, clearly opposing duodenum and colon. A thinner layer ($p < 0.01$) was observed in duodenum and a higher cell density in jejunum ($p < 0.05$). Villin-1 expression intensity was lower in colon ($p < 0.05$) and neuroendocrine cell density was higher in duodenum ($p < 0.001$). Goblet cell density increased along the digestive tract (lower for duodenum ($p < 0.05$) and higher in colon ($p < 0.01$)), while the proportion of acid vs. neutral mucins decreased (higher in duodenum ($p < 0.001$) and lower in colon ($p < 0.05$)). These observations are in accordance with published data on these pig tissues (Świąch *et al.*, 2019).

In our culture conditions, ileum organoids appeared different from all other gut-derived organoids (Figure 2B) in showing higher cell density ($p < 0.01$) and higher goblet cell and neuroendocrine cell density ($p < 0.001$ and $p < 0.05$, respectively). Jejunum organoids showed also lower goblet cell density ($p < 0.05$). Goblet cells were found at high levels in ileum organoids compared to jejunum and duodenum organoids. In colon organoids, goblet cells were also found at high levels although at a lower level than in ileum. Interestingly, in the latter, mucins were more acid than in colon organoids, as observed in the original tissues.

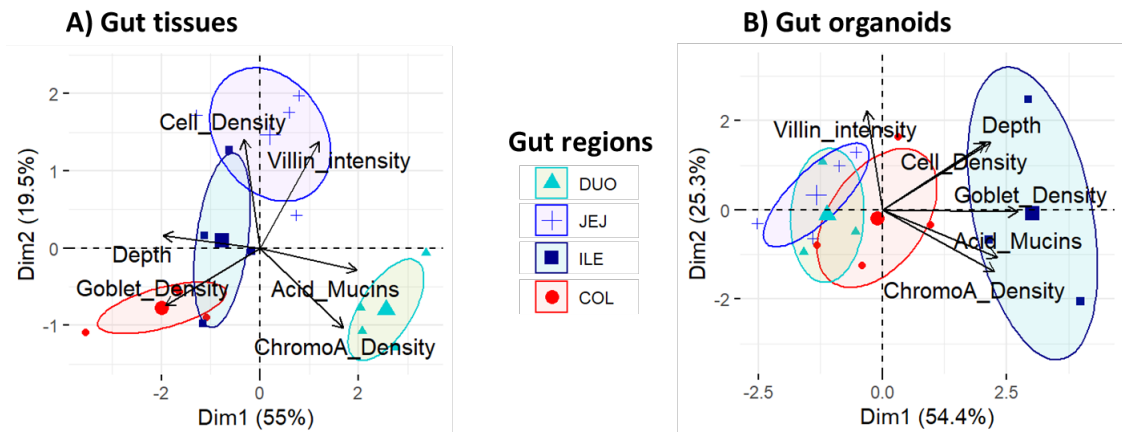


Figure 2. Principal component analyses of (A) gut tissues from different gut regions (duodenum, jejunum, ileum and colon), and (B) their derived organoids after 7 days of culture. Histological and immunohistochemical parameters included: depth of the layer (Depth), cell density (Cell_Density), goblet cell density (Goblet_Density), neuroendocrine cell density (ChromoA_Density), villin-1 expression intensity (Villin_Intensity) and percentage of acid mucins (Acid_Mucins).

We are currently gaining insights into this comparison using transcriptomics to decipher to what extent pig organoids have retained transcript expression and functional pathways of the epithelia of the different gut segments.

References

- Beaumont M., Blanc F., Cherbuy C., Egidy G., Giuffra E. *et al.* (2021) *Vet. Res.* 52(1):1-15. <https://doi.org/10.1186/s13567-021-00909-x>
- Clark E.L., Archibald A.L., Daetwyler H.D., Groenen M.A.M., Harrison P.W. *et al.* (2020) *Genome Biol.* 21(1):285. <https://doi.org/10.1186/s13059-020-02197-8>
- Clevers H. (2016) *Cell* 165(7):1586-1597. <https://doi.org/10.1016/j.cell.2016.05.082>
- Criss Z.K., Bhasin N., Di Rienzi S.C., Rajan A., Deans-Fielder K. *et al.* (2021) *Physiol. Genomics* 53(11):486-508. <https://doi.org/10.1152/physiolgenomics.00061.2021>
- Gehling K., Parekh S., Schneider F., Kirchner M., Kondylis V. *et al.* (2021) *bioRxiv* 2021.11.22.469588. <https://doi.org/10.1101/2021.11.22.469588>
- Li L., Fu F., Guo S., Wang H., He X. *et al.* (2019) *J Virol* 93(5):e01682-18. <https://doi.org/10.1128/JVI.01682-18>
- Mohammadi S., Morell-Perez C., Wright C.W., Wyche T.P., White C.H. *et al.* (2021) *Stem Cell Reports* 16(9):2364-2378. <https://doi.org/10.1016/j.stemcr.2021.07.016>
- Świąch E., Tuśnio A., Barszcz M., Taciak M., and Siwiak E. (2019) *J Anim Physiol Anim Nutr.* 103(3):894-905. <https://doi.org/10.1111/jpn.13086>
- Tsai Y.H., Czerwinski M., Wu A., Dame M.K., Attili D. *et al.* (2018) *Cell. Mol. Gastroenterol. Hepatol.* 6(2):218-222. <https://doi.org/10.1016/j.jcmgh.2018.04.008>
- van der Hee B., Loonen L.M.P., Taverne N., Taverne-thiele J.J., Smidt H. *et al.* (2018) *Stem Cell Res.* 28:165-171. <https://www.doi.org/10.1016/j.scr.2018.02.013>
- van der Hee B., Madsen O., Vervoort J., Smidt H., and Wells J.M. (2020) *Front. Cell Dev. Biol.* 8. <https://www.doi.org/10.3389/fcell.2020.00375>